

Increased carrier generation rate in Si nanocrystals in SiO₂ investigated by induced absorption

W. D. A. M. de Boer,^{1,a)} M. T. Trinh,¹ D. Timmerman,¹ J. M. Schins,² L. D. A. Siebbeles,² and T. Gregorkiewicz¹

¹Van der Waals-Zeeman Institute, University of Amsterdam, Science Park 904, Amsterdam 1098 XH, The Netherlands

²Department of Chemical Engineering, Delft University of Technology, Julianalaan 136, Delft 2628 BL, The Netherlands

(Received 16 June 2011; accepted 14 July 2011; published online 5 August 2011)

We report on investigations of optical generation of carriers in Si nanocrystals embedded in SiO₂ matrix by time-resolved induced absorption technique. Results obtained for excitation below and above twice the bandgap energy $h\nu < 2E_g$ and $h\nu > 2E_g$ show very similar decay characteristics (within $\tau_{\text{resolution}} \approx 100$ fs). When intensity of the signal is correlated to number of generated excitons, it is found that for the high photon energy excitation, carrier generation rate is considerably enhanced. These results are discussed in terms of carrier multiplication reported previously for semiconductor nanocrystals and photoluminescence quantum yield measurements for similar materials. © 2011 American Institute of Physics. [doi:10.1063/1.3622308]

In the last two decades, silicon nanocrystals (Si-NCs) have been frequently investigated. Following intensive studies, exciting application prospects for Si-NCs have been identified in photonics,¹ medicine,² and in photovoltaics (PV).³ A particularly interesting feature of semiconductor NCs relates to the effect of quantum confinement on the impact excitation—a process in which a high energy free carrier relaxes by inducing band-to-band transitions. In that way, additional electron-hole pairs are created, and the process is frequently termed *carrier multiplication* (CM). For PV applications, generation of multiple electron-hole pairs by absorption of a single high-energy photon enables more efficient light-to-electricity conversion, as part of the energy otherwise lost to heat is converted into free carrier population.⁴ It has been suggested that in NCs, the CM rate could be enhanced and its threshold energy reduced due to (1) increased Coulomb interaction between carriers, (2) relaxation of momentum conservation, and (3) possible reduction of the carrier-phonon scattering rate.⁵ In line with these expectations, enhanced CM has been reported for NCs of different semiconducting materials^{6–8} including colloidal Si-NCs.⁹ These results were typically obtained from investigations of carrier dynamics by induced absorption (IA), where the CM effect was identified by a fast decay component appearing due to Auger interaction of multiple excitons within the same NC.

Here, we report on investigations of carrier generation rate upon optical absorption in dense solid-state dispersions of small Si-NCs of high crystalline quality in a SiO₂-matrix with average diameters $d_{\text{NC}} = 2.5, 3, 4,$ and 5.5 nm. The samples were prepared by radio-frequency co-sputtering followed by high-temperature annealing. Details of sample preparation can be found in Ref. 10. Samples were optically characterized by photoluminescence (PL), using a standard

configuration featuring tunable pulsed (5 ns) excitation in the visible and time-resolved detection with a photomultiplier tube. For IA experiments, a conventional pump-probe setup was employed, comprising an optical parametric amplifier, pumped by a chirped-pulse amplified Ti:Sapphire laser, with a repetition rate of $f = 1$ kHz and ~ 100 fs resolution. IA dynamics recorded at the two available different probing photon energies ($E_{\text{det}} = 1.8$ eV and $E_{\text{det}} = 0.95$ eV) showed similar characteristics. Dimensions of the pump spot size were chosen to be considerably larger than those of the secondary pulse to assure complete overlap during the entire experiment. For excitation, pump photon energies of $E_{\text{exc}} = 2.48$ eV and $E_{\text{exc}} = 4.66$ eV were used. For all the investigated samples, this corresponds to below and above twice the optical bandgap energy, respectively (see Table I). Based on results reported previously for other materials, we expect that the chosen pumping energies provide excitation below (2.48 eV) and above (4.66 eV) CM-threshold, for all samples. The experiments were performed at room temperature.

Figure 1 illustrates optical properties of the sample with average diameter of $d_{\text{NC}} = 5.5$ nm. In Fig. 1(a), the steady-state PL spectrum is shown, centered around $E_{\text{max}} = 1.26$ eV. The PL decay dynamics, recorded at the maximum intensity of the PL spectrum—panel (b)—reveals a characteristic decay time of $\tau_{\text{PL}} \approx 230$ μs , typical for Si-NCs of this size

TABLE I. Sample characteristics. In the first column, the average NC diameter of the different samples are shown, with their corresponding optical energy bandgap (second column). The third and fourth columns display the two excitation photon energies relative to the NC bandgap.

| d_{NC} [nm] | E_{gap} [eV] | $E_{\text{exc}} = 2.48 \text{ eV } N \times E_{\text{gap}}$ | $E_{\text{exc}} = 4.66 \text{ eV } n \times E_{\text{gap}}$ |
|----------------------|-----------------------|---|---|
| 2.5 | 1.65 | 1.50 | 2.8 |
| 3.0 | 1.59 | 1.56 | 2.9 |
| 4.0 | 1.44 | 1.77 | 3.2 |
| 5.5 | 1.26 | 1.97 | 3.7 |

^{a)}Electronic mail: W.D.A.M.deBoer@uva.nl. Tel.: +31-(0)20-525-6646. Fax: +31-(0)20-525-5788.

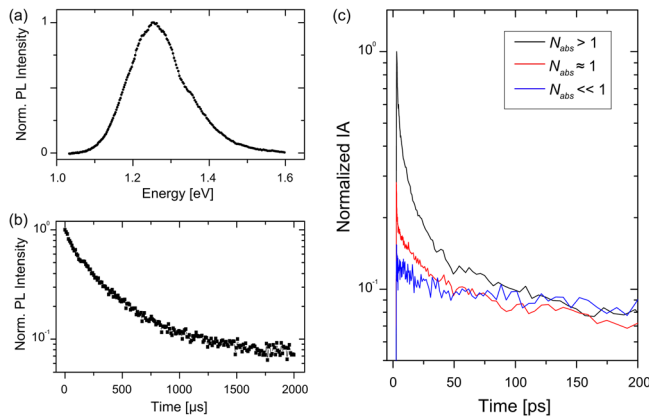


FIG. 1. (Color online) Characteristics of the sample with an average NC diameter of $d_{\text{NC}} = 5.5$ nm. (a) (Normalized) steady-state PL spectrum, centered around $E_{\text{max}} = 1.26$ eV, obtained under pulsed excitation of $E_{\text{exc}} = 2.75$ eV. (b) PL dynamics recorded at E_{max} , with a characteristic decay time of $\tau_{\text{PL}} \approx 230$ μs . (c) IA transient under increasing excitation photon fluences ($E_{\text{exc}} = 2.48$ eV), resulting in average number of excitons per NC $N_{\text{abs}} \ll 1$ (blue), $N_{\text{abs}} \approx 1$ (red), and $N_{\text{abs}} > 1$ (black), in a 200 ps time window.

embedded in SiO_2 .¹¹ In panel (c), IA transients obtained under $E_{\text{exc}} = 2.48$ eV pumping, below the expected CM threshold, with various photon fluences are shown in a 1 ns time window. These feature a multi-exponential picosecond decay, superimposed on a slower background, which can be related to radiative recombination of excitons. As can be seen, the relative contribution of the fast decaying component of the IA signal increases with the pump power; this can be predominantly attributed to Auger interaction of multiple excitons appearing in the same NCs at higher pump fluence, as a consequence of absorption of several photons. In order to avoid such non-linear effects and to establish dynamics characteristic for a single exciton per NC, the measurements need to be conducted under low excitation photon fluence, where the average number of absorbed photons per NC is much smaller than 1 (i.e., $N_{\text{abs}} \ll 1$). (We note that even for the case of $N_{\text{abs}} = 0.5$, still $\sim 23\%$ of excited NCs have absorbed 2 or more photons, as a result of Poissonian statistics of excitation). In the present study, rather than relying on imprecise estimation of number of absorbed photons per NC by estimating the absorption cross-section of individual NCs, the low excitation fluence regime is established experimentally by gradually lowering the pump power. This is demonstrated in Fig. 2(a); Here, the lowest transient corresponds to the fluence range in which only the amplitude of the IA signal changes, and not its decay characteristics.¹² As can be seen, the single exciton dynamics in Si-NCs investigated here features a multi-exponential decay. This is characteristic for these materials and originates from the simultaneous presence of different relaxation channels, such as efficient trapping and other fast (non-radiative) processes inherent for Si in view of its indirect bandgap.¹³

In order to find the effect of excitation photon energy on carrier generation, we compare IA signals for sub- and super-CM-threshold excitation, normalized to equal number of absorbed photons. The IA signal is proportional to the number of excitons generated by the pump pulse and available in the sample at a particular moment of probing. The

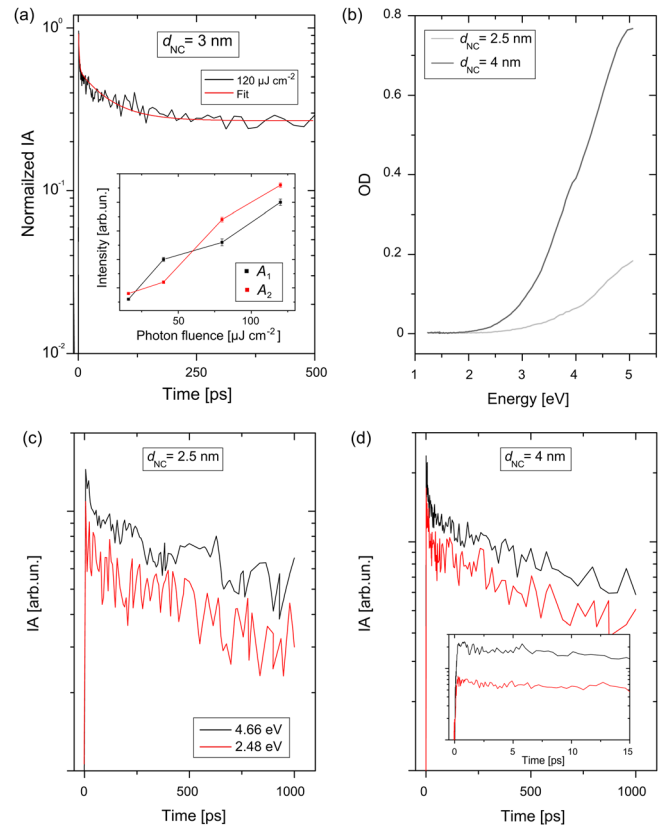


FIG. 2. (Color online) (a) IA transients for the sample with average diameter of (a) $d_{\text{NC}} = 3$ nm under pumping of $j = 120$ $\mu\text{J cm}^{-2}$ in a 1 ns time window. Inset: A_1 and A_2 , the amplitudes of the two time constants found with a bi-exponential fitting procedure, are plotted vs. photon fluence. (b) OD for two different samples with average NC diameter of $d_{\text{NC}} = 2.5$ nm and $d_{\text{NC}} = 4$ nm, in the range of 1.25-5 eV. (c) IA transients for two excitation photon energies of $E_{\text{exc}} = 2.48$ eV (red) and $E_{\text{exc}} = 4.66$ eV (black), under excitation condition of $N_{\text{abs}} \ll 1$ and scaled for the same number of absorbed (pump) photons N_{abs} for sample with average diameter of $d_{\text{NC}} = 2.5$ nm. (d) IA transients for two excitation photon energies of $E_{\text{exc}} = 2.48$ eV (red) and $E_{\text{exc}} = 4.66$ eV (black), under excitation condition of $N_{\text{abs}} \ll 1$ and scaled for the same number of absorbed (pump) photons N_{abs} for sample with average diameter of $d_{\text{NC}} = 4$ nm. In the inset, the first 15 ps are shown, indicating similar build up characteristics for both excitations.

total number of pump photons per pulse absorbed in the sample, $N_{\text{abs}}^{\text{tot}}$, can be expressed as the difference between the photon fluence before and after passing through the sample of thickness L , $j(0) - j(L)$ —see Eq. (1). Using Lambert-Beer law, describing the exponential decrease of the number of photons with penetration depth and the notion that excitation photon fluence (or flux) follows the same dependence, the relation can be rewritten as function of the initial photon fluence before the sample, $j(0)$, and the optical density (OD):

$$N_{\text{abs}}^{\text{tot}} \propto j(0) - j(L) = j(0)(1 - e^{(-\text{OD} \ln[10])}). \quad (1)$$

In the usual approach, the number of excitons generated by the pump pulse, and, therefore, the amplitude of the IA signal, is correlated with the (average) number of absorbed photons per NC, N_{abs} . This is evaluated by taking the product of the excitation photon fluence and the absorption cross section σ_{abs} . The latter is derived from the linear absorption, applying various scaling factors which either cannot be accurately or directly measured (e.g., NC diameter or field

factor). As a result, N_{abs} is frequently over- or underestimated. To avoid these hurdles, in the present approach, we base our analysis on parameters which can be determined directly and independently: $j(0)$ and OD . The latter is measured using a UV-VIS Lambda 900 spectrometer in combination with an integrating sphere, so that scattering effects are accounted for. In Fig. 2(b), the OD is shown for two samples, with average diameter of $d_{\text{NC}} = 2.5$ nm (light grey) and $d_{\text{NC}} = 4$ nm (dark grey), corrected for the (separately measured) possible absorption in the substrate layer.

Next, in order to remove the proportionality in expression (1), we evaluate the ratio of the total number of absorbed photons $N_{\text{abs}}^{\text{tot}}$ for the two excitation conditions, above ($E_{\text{exc}} = 4.66$ eV) and below ($E_{\text{exc}} = 2.48$ eV) the CM-threshold, $\frac{N_{\text{abs}}^{\text{tot}}(466\text{eV})}{N_{\text{abs}}^{\text{tot}}(248\text{eV})}$:

$$\frac{N_{\text{abs}}^{\text{tot}}(466\text{eV})}{N_{\text{abs}}^{\text{tot}}(248\text{eV})} = \frac{j(0)_{4.66\text{eV}}(1 - e^{(-OD(4.66\text{eV})\ln[10])})}{j(0)_{2.48\text{eV}}(1 - e^{(-OD(2.48\text{eV})\ln[10])})}. \quad (2)$$

Subsequently, the measured IA signal is scaled with the correction factor given by Eq. (2); This is done for the samples with average NC diameters of $d_{\text{NC}} = 2.5$ nm and $d_{\text{NC}} = 4$ nm, shown in Figs. 2(c) and 2(d). Here, the red trace is the data recorded under excitation photon energy of $E_{\text{exc}} = 2.48$ eV and the black for the high photon energy condition of $E_{\text{exc}} = 4.66$ eV, respectively. First, we note that the IA transients taken at different pumping photon energies are very similar, with no evidence of a component related to Auger interaction between multiple excitons in the same NC for the high photon energy excitation. In addition, it can also be inferred that the possible effect of photocharging is either negligible or occurs with the same rate for below and above CM-threshold pumping. The photocharging effect could give rise to an additional ps component (or increase of the amplitude of the initial fast component), by which CM-rates can easily be overestimated.¹² After scaling of the IA signals to equal number of absorbed photons in the sample, the IA amplitude for the high photon energy excitation (for both samples) is a factor ~ 1.5 higher. Similar enhancement is observed for all samples investigated in this study. It should be noted that possible difference in scattering for the two excitations will only increase this number. These findings— increase of IA signal intensity, in combination with the absence of Auger-related components in dynamics, evidence that CM occurs at high pumping photon energy but does not lead to strong interaction between generated carriers. This would happen if multiple carriers generated by a high-energy photon separate before efficient Auger interaction sets in, possibly into different neighboring NCs, either during or right after photon absorption. A similar conclusion has been reached from investigations of PL quantum yield (QY) on similar samples;³ In that case, a threshold enhancement of QY at higher pumping photon energies has been concluded, suggesting increase of concentration of singly excited NCs. (We note that for PL measurements, the lifetime of generated excitons has to be sufficiently long in order to allow for their radiative recombination).

While microscopic models of CM are still under dispute, it follows from the available experimental results (and theo-

retical assessments) that the process occurs on an ultrafast (instantaneous) timescale.¹⁴ The current study confirms that: within the ~ 100 fs resolution of the IA experiment, no difference in carrier dynamics is found between below- and above-threshold excitation. This is demonstrated in Fig. 2(d), where the corrected IA transients are shown for the sample with the average diameter of $d_{\text{NC}} = 4$ nm in a 15 ps time window, revealing no apparent difference in rise time for the two excitation conditions. The ultrafast buildup of signal is consistent with previous reports on transient IA (Ref. 15) and also PL (Refs. 16 and 17) investigations of Si-NC systems. From high resolution IA transients, we conclude that the CM process takes place on the time scale shorter than ~ 100 fs, which explains why it can compete with carrier cooling proceeding on picosecond time scale.¹⁸

In conclusion, using time-resolved IA, we have obtained evidence for enhancement of carrier generation rate at high pumping photon energy in dense solid state dispersions of Si-NCs in SiO₂. In comparison to the previous report on CM in colloidal Si-NCs⁹ in the materials investigated in this study, the multiple excitons generated by high energy photons ($h\nu > 2E_g$) do not undergo fast Auger recombination. We suggest that this is related to close proximity of Si-NC allowing for a possible separation of multiple excitons created in the CM process

The authors acknowledge M. Fujii (Kobe University) for sharing the expertise on preparation of sputtered layers. This work has been financially sponsored by Stichting voor de Technologische Wetenschappen (STW) and Nederlandse Organisatie voor Wetenschappelijk Onderzoek (NWO).

¹L. Pavesi, L. D. Negro, C. Mazzoleni, G. Franzò, and F. Priolo, *Nature* **408**, 440 (2000).

²J.-H. Park, L. Gu, G. von Maltzahn, E. Ruoslahti, S. N. Bhatia, and M. J. Sailor, *Nature Mater.* **8**, 331 (2009).

³D. Timmerman, I. Izuddin, P. Stallinga, I. N. Yassievich, and T. Gregorkiewicz, *Nat. Photonics* **2**, 105 (2008).

⁴A. J. Nozik, *Nano Lett.* **10**, 2735 (2010).

⁵A. J. Nozik, *Physica E* **14**, 115 (2002).

⁶R. D. Schaller, M. A. Petruska, and V. I. Klimov, *Appl. Phys. Lett.* **87**, 25102 (2005).

⁷M. T. Trinh, L. Polak, J. M. Schins, A. J. Houtepen, R. Vaxenburg, G. I. Maikov, G. Grimbom, A. G. Midgett, J. M. Luther, M. C. Beard, A. J. Nozik, M. Bonn, E. Lifshitz, and L. D. A. Siebbeles, *Nano Lett.* **11**, 1623 (2011).

⁸J. B. Sambur, T. Novet, and B. A. Parkinson, *Science* **330**, 63 (2002).

⁹M. Beard, K. P. Knutsen, Y. Pingrong, J. M. Luther, Q. Song, W. K. Metzger, R. J. Ellingson, and A. J. Nozik, *Nano Lett.* **7**, 2506 (2007).

¹⁰S. Takeoka, M. Fujii, and S. Hayashi, *Phys. Rev. B* **62**, 16820 (2000).

¹¹D. Timmerman, I. Izuddin, and T. Gregorkiewicz, *Phys. Status Solidi A* **1**, 183 (2010).

¹²M. T. Trinh, A. J. Houtepen, J. M. Schins, T. Hanrath, J. Pirus, W. Knulst, A. P. L. M. Goossens, and L. D. A. Siebbeles, *Nano Lett.* **8**, 1713 (2008).

¹³F. Trójánek, K. Neudert, P. Maly, K. Dohnalová, and I. Pelant, *J. Appl. Phys.* **99**, 116108 (2006).

¹⁴R. D. Schaller, V. M. Agranovich, and V. I. Klimov, *Nat. Phys.* **1**, 198 (2005).

¹⁵E. Lioudakis, A. Othonos, and A. G. Nassiopoulou, *Appl. Phys. Lett.* **90**, 171103 (2007).

¹⁶W. de Boer, H. Zhang, and T. Gregorkiewicz, *Mater. Sci. Eng. B* **159–160**, 190 (2009).

¹⁷M. Sykora, L. Mangolini, R. D. Schaller, U. Kortshagen, D. Jurbergs, and V. I. Klimov, *Phys. Rev. Lett.* **100**, 067401 (2008).

¹⁸W. D. A. M. de Boer, D. Timmerman, K. Dohnalová, I. N. Yassievich, H. Zhang, W.-J. Buma, and T. Gregorkiewicz, *Nat. Nanotechnol.* **5**, 878 (2010).